

**Strange quark matter in a chiral SU(3) quark mean field model**

P. Wang, V. E. Lyubovitskij, Th. Gutsche, and Amand Faessler

*Institut für Theoretische Physik, Universität Tübingen, Auf der Morgenstelle 14, D-72076 Tübingen, Germany*

(Received 23 May 2002; published 31 January 2003)

We apply the chiral SU(3) quark mean field model to investigate strange quark matter. The stability of strange quark matter with a different strangeness fraction is studied. The interaction between quarks and vector mesons destabilizes the strange quark matter. If the strength of the vector coupling is the same as in hadronic matter, strangelets cannot be formed. For the case of  $\beta$  equilibrium, there is no strange quark matter that can be stable against hadron emission even without vector meson interactions.

DOI: 10.1103/PhysRevC.67.015210

PACS number(s): 11.30.Rd, 12.39.Ki, 14.65.Bt, 24.85.+p

**I. INTRODUCTION**

Strange quark matter has attracted a lot of interest since Bodmer [1] and, later on, Witten [2] suggested that it could be absolutely stable even at zero temperature and pressure. The investigation of such a possibility is relevant not only for high energy physics, but also for astrophysics. For example, the core of a neutron star may be composed of quark matter. The possible existence of strange stars that are made entirely of deconfined  $u$ ,  $d$ , and  $s$  quarks is one of the most intriguing aspects of modern astrophysics. There have been some reports on events with  $A \approx 350$ – $500$  and  $Z \approx 10$ – $20$  in cosmic ray experiments [3], the so-called exotic cosmic ray events. Also, recent studies have shown that x-ray burst sources are likely strange star candidates [4,5]. It is also interesting to produce strange quark matter (strangelets) in the laboratory because they could serve as a signature of the quark-gluon-plasma formation which is a direct demonstration of QCD [6]. Many ultrarelativistic heavy-ion collision experiments at Brookhaven and CERN [7] are proposed to search for (meta)stable lumps of such kind of strangelets. Recently, Ardouin *et al.* [8] presented a novel method that can be applied to characterize the possible existence of a strange quark matter distillation process in heavy-ion collisions. Up to now, there is no experiment which confirms the existence of strangelets. For example, the E864 collaboration found that there is no evidence for strangelet production in 11.5 GeV/ $c$  per nucleon Au+Pb collisions [9].

Besides the experimental efforts, there are also a lot of theoretical investigations of the stability of strange quark matter. The earliest discussions are based on the MIT bag model [10] that assumes that quarks are confined by a phenomenological bag. Within the bag, quarks are asymptotically free. Calculations [11] within this model indicate that there is a range of parameters in which strange quark matter is absolutely stable, i.e., the energy per baryon is less than 930 MeV. The stability of strange quark matter with finite volume (strangelets) was also discussed in the MIT bag model. Chin and Kerman [12] proposed that multi-quark states with large strangeness fraction (large negative charge) may be metastable. Berger and Jaffe [13] discussed the surface correction for the strangelets, where they found that the surface tension destabilizes strangelets. In response to the work of Berger and Jaffe, Schaffner *et al.* [14] found that strangelets can be stabilized by shell effects and that they

have large negative charges too. The curvature contribution was considered by Madsen [15], which is dominant for strangelets with small baryon numbers. Though the bag model is simple, it is an incomplete description of confinement. Results from lattice calculations [16] show that quark matter does not become asymptotically free and some hadronic degrees of freedom remain within the quark matter immediately after the phase transition. Fowler, Raha, and Weiner [17] suggested another description of the confinement mechanism via the introduction of a density-dependent quark mass. This quark mass-density-dependent (QMDD) model was first employed to study the properties of ordinary quark matter [17] and then applied to the investigation of strange quark matter [18]. As was pointed in our recent paper [19], their thermodynamic treatment was not correct. We re-considered strange quark matter in the self-consistent quark mass-density-dependent model and found a region of parameters in which the strange quark matter is absolutely stable.

In the QMDD model, the concept of a density-dependent quark mass has no dynamical origin. In recent years, some approaches for strange quark matter based on dynamical models were developed. Alberico *et al.* [20] utilized the colored dielectric model to calculate the energy per baryon of strange quark matter. They found that while the double minimum version of the colored dielectric model allowed the existence of strangelets, the single minimum version of this model excluded the possibility. Stability of strange quark matter was also investigated using the effective four-quark interactions [21], the SU(3) Nambu-Jona-Lasinio (NJL) model with and without four-quark-vector-type interactions [22,23]. In studying hadronic matter, we proposed a chiral SU(3) quark mean field model. This chiral quark model was applied to investigate the properties of strange hadronic matter and multistrange hadronic systems [24,25]. In this paper, we want to use this model to discuss the stability of strange quark matter. The difference between quark and hadronic matter is that in quark matter, the  $u$ ,  $d$ ,  $s$  quarks are deconfined and not combined into baryons by the confining potential.

The paper is organized as follows. In Sec. II, we introduce the basic model features. We apply the model to investigate strange quark matter in Sec. III. The numerical calculations are discussed in Sec. IV. Finally, main conclusions are drawn in Sec. V.

## II. THE MODEL

Our considerations are based on the chiral SU(3) quark mean field model (for details, see Refs. [24,25]). For completeness, we introduce the main concepts of the model in this section. In the chiral limit, the quark field  $q$  can be split into left- and right-handed parts  $q_L$  and  $q_R$ :  $q = q_L + q_R$ . Under  $SU(3)_L \times SU(3)_R$ , they transform as

$$q'_L = L q_L, \quad q'_R = R q_R. \quad (1)$$

The spin-0 mesons are written in the compact form

$$M(M^+) = \Sigma \pm i\Pi = \frac{1}{\sqrt{2}} \sum_{a=0}^8 (\sigma^a \pm i\pi^a) \lambda^a, \quad (2)$$

where  $\sigma^a$  and  $\pi^a$  are the nonets of scalar and pseudoscalar mesons, respectively,  $\lambda^a (a=1, \dots, 8)$  are the Gell-Mann matrices, and  $\lambda^0 = \sqrt{\frac{2}{3}}I$ . Plus and minus signs correspond to  $M$  and  $M^+$ . Under chiral SU(3) transformations,  $M$  and  $M^+$  transform as  $M \rightarrow M' = LMR^+$  and  $M^+ \rightarrow M'^+ = RM^+L^+$ . As for the spin-0 mesons, the spin-1 mesons are set up in a similar way as

$$l_\mu(r_\mu) = \frac{1}{2}(V_\mu \pm A_\mu) = \frac{1}{2\sqrt{2}} \sum_{a=0}^8 (v_\mu^a \pm a_\mu^a) \lambda^a. \quad (3)$$

They transform as  $l_\mu \rightarrow l'_\mu = Ll_\mu L^+$ ,  $r'_\mu = Rr_\mu R^+$ . These matrices can be written in a form where the physical states are explicit. For the scalar and vector nonets, the expressions are

$$\Sigma = \frac{1}{\sqrt{2}} \sum_{a=0}^8 \sigma^a \lambda^a = \begin{pmatrix} \frac{1}{\sqrt{2}}(\sigma + a_0^0) & a_0^+ & K^{*+} \\ a_0^- & \frac{1}{\sqrt{2}}(\sigma - a_0^0) & K^{*0} \\ K^{*-} & \bar{K}^{*0} & \zeta \end{pmatrix}, \quad (4)$$

$$V_\mu = \frac{1}{\sqrt{2}} \sum_{a=0}^8 v_\mu^a \lambda^a = \begin{pmatrix} \frac{1}{\sqrt{2}}(\omega_\mu + \rho_\mu^0) & \rho_\mu^+ & K_\mu^{*+} \\ \rho_\mu^- & \frac{1}{\sqrt{2}}(\omega_\mu - \rho_\mu^0) & K_\mu^{*0} \\ K_\mu^{*-} & \bar{K}_\mu^{*0} & \phi_\mu \end{pmatrix}. \quad (5)$$

Pseudoscalar and pseudovector nonet mesons can be written in the same way.

The total effective Lagrangian for the description of strange quark matter is given by

$$\mathcal{L}_{\text{eff}} = \mathcal{L}_{q0} + \mathcal{L}_{qM} + \mathcal{L}_{\Sigma\Sigma} + \mathcal{L}_{VV} + \mathcal{L}_{\chi SB} + \mathcal{L}_{\Delta m_s} + \mathcal{L}_h. \quad (6)$$

It contains the free part for massless quarks  $\mathcal{L}_{q0} = \bar{q}i\gamma^\mu \partial_\mu q$ , the quark-meson field interaction term

$$\mathcal{L}_{qM} = g_s(\bar{q}_L M q_R + \bar{q}_R M^+ q_L) - g_v(\bar{q}_L \gamma^\mu l_\mu q_L + \bar{q}_R \gamma^\mu r_\mu q_R), \quad (7)$$

the chiral-invariant scalar meson  $\mathcal{L}_{\Sigma\Sigma}$  and vector meson  $\mathcal{L}_{VV}$  self-interaction terms in the mean field approximation [24,26]

$$\begin{aligned} \mathcal{L}_{\Sigma\Sigma} = & -\frac{1}{2}k_0\chi^2(\sigma^2 + \zeta^2) + k_1(\sigma^2 + \zeta^2)^2 + k_2\left(\frac{\sigma^4}{2} + \zeta^4\right) \\ & + k_3\chi\sigma^2\zeta - k_4\chi^4 - \frac{1}{4}\chi^4 \ln\left(\frac{\chi^4}{\chi_0^4}\right) + \frac{\delta}{3}\chi^4 \ln\left(\frac{\sigma^2\zeta}{\sigma_0^2\zeta_0}\right), \end{aligned} \quad (8)$$

$$\begin{aligned} \mathcal{L}_{VV} = & \frac{1}{2}\frac{\chi^2}{\chi_0^2}(m_\omega^2\omega^2 + m_\rho^2\rho^2 + m_\phi^2\phi^2) \\ & + g_4(\omega^4 + 6\omega^2\rho^2 + \rho^4 + 2\phi^4), \end{aligned} \quad (9)$$

where  $\delta = 6/33$ ;  $\sigma_0$ ,  $\zeta_0$ , and  $\chi_0$  are the vacuum values of the mean fields  $\sigma$ ,  $\zeta$ , and  $\chi$  and the three terms  $\mathcal{L}_{\chi SB}$ ,  $\mathcal{L}_{\Delta m_s}$ , and  $\mathcal{L}_h$  which explicitly break the chiral symmetry. The Lagrangian (8) contains a new field, a dilaton field  $\chi$ , which is not a glueball field in our approach. In this view, we follow the ideas of Ref. [27] and relate the field  $\chi$  to a glueball field  $h$  as

$$\chi^4 = \chi_0^4 + Zh, \quad (10)$$

where  $Z$  is an appropriate dimensional parameter. In Eq. (9), the masses of vector mesons are density dependent which are expressed as

$$m_\omega^2 = m_\rho^2 = \frac{m_v^2}{1 - \frac{1}{2}\mu\sigma^2} \quad \text{and} \quad m_\phi^2 = \frac{m_v^2}{1 - \mu\zeta^2},$$

where  $m_v = 673.6$  MeV and  $\mu = 2.34$  fm<sup>2</sup> are chosen to get  $m_\omega = 783$  MeV and  $m_\phi = 1020$  MeV. Chiral symmetry requires the following basic relations for the quark-meson coupling constants:

$$\begin{aligned} \frac{g_s}{\sqrt{2}} = g_{a_0}^u = -g_{a_0}^d = g_\sigma^u = g_\sigma^d = \dots = \frac{1}{\sqrt{2}}g_\zeta^s, \\ g_{a_0}^s = g_\sigma^s = g_\zeta^u = g_\zeta^d = 0, \end{aligned} \quad (11)$$

$$\frac{g_v}{2\sqrt{2}} = g_{\rho^0}^u = -g_{\rho^0}^d = g_\omega^u = g_\omega^d = \dots = \frac{1}{\sqrt{2}}g_\phi^s,$$

$$g_\omega^s = g_{\rho^0}^s = g_\phi^u = g_\phi^d = 0. \quad (12)$$

Note, the values of  $\sigma_0$ ,  $\zeta_0$ , and  $\chi_0$  are determined later from Eqs. (26) to (28). Particularly, the parameters  $\sigma_0$  and  $\zeta_0$  are

TABLE I. Parameters of sets *A*, *B*, and *C* of the model.

Set	$k_0$	$k_1$	$k_2$	$k_3$	$k_4$	$g_s$	$g_v$	$g_4$	$h_1$	$h_2$
<i>A</i>	4.94	2.12	-10.16	-5.38	-0.06	4.76	10.92	37.5	-2.20	3.24
<i>B</i>	3.83	2.64	-10.16	-3.40	-0.18	4.76	10.13	0.0	-2.03	2.55
<i>C</i>	4.21	2.26	-10.16	-4.38	-0.13	4.76	10.37	7.5	-2.07	3.16

expressed through the pion ( $F_\pi=93$  MeV) and the kaon ( $F_K=115$  MeV) leptonic decay constants as

$$\sigma_0 = -F_\pi, \quad \zeta_0 = \frac{1}{\sqrt{2}}(F_\pi - 2F_K). \quad (13)$$

The Lagrangian  $\mathcal{L}_{\chi SB}$  generates the nonvanishing masses of pseudoscalar mesons

$$\mathcal{L}_{\chi SB} = \frac{\chi^2}{\chi_0^2} \left[ m_\pi^2 F_\pi \sigma + \left( \sqrt{2} m_K^2 F_K - \frac{m_\pi^2}{\sqrt{2}} F_\pi \right) \zeta \right] \quad (14)$$

leading to a nonvanishing divergence of the axial currents which satisfy the partially conserved axial-vector current (PCAC) relations for  $\pi$  and  $K$  mesons. Pseudoscalar and scalar mesons and also the dilaton field  $\chi$  obtain the masses by spontaneous breaking of the chiral symmetry in the Lagrangian (8). The masses of  $u$ ,  $d$ , and  $s$  quarks are generated by the vacuum expectation values of the two scalar mesons  $\sigma$  and  $\zeta$ . To obtain the correct constituent mass of the strange quark, an additional mass term should be added

$$\mathcal{L}_{\Delta m_s} = -\Delta m_s \bar{q} S q, \quad (15)$$

where  $S = \frac{1}{3}(I - \lambda_8 \sqrt{3}) = \text{diag}(0, 0, 1)$  is the strangeness quark matrix. Finally, the quark masses are given by

$$m_u = m_d = -\frac{g_s}{\sqrt{2}} \sigma_0, \quad m_s = -g_s \zeta_0 + \Delta m_s. \quad (16)$$

The parameters  $g_s = 4.76$  and  $\Delta m_s = 29$  MeV are determined from  $m_q = 313$  MeV and  $m_s = 490$  MeV. In order to obtain reasonable hyperon potentials in hadronic matter, we include the additional coupling between strange quarks and scalar mesons  $\sigma$  and  $\zeta$  [24]. This term is expressed as

$$\mathcal{L}_h = (h_1 \sigma + h_2 \zeta) \bar{s} s. \quad (17)$$

In our calculations, we consider three sets of free parameters: set *A*, set *B*, and set *C*. Though parameter set *C* is preferred for hadronic matter, we will discuss strange quark matter with these three sets for completeness. The values of free model parameters  $k_i (i=0, \dots, 4)$ ,  $g_s, g_v, g_4, h_1$ , and  $h_2$  are given in Table I. We also list the values of the meson masses used in the calculation. The masses of pseudoscalar and vector mesons are the same for all three sets:  $m_\pi = 139$  MeV,  $m_K = 496$  MeV,  $m_\eta = 540.1$  MeV,  $m'_\eta = 961.9$  MeV,  $m_\omega = m_\rho = 783$  MeV, and  $m_\phi = 1020$  MeV. The masses of scalar mesons  $\sigma$  and  $\zeta$  and the mass and vacuum expectation value of the dilaton field  $\chi$  are

$$\begin{aligned} \text{set } A: \quad & m_\sigma = 417.5 \text{ MeV}, \quad m_\zeta = 1170.1 \text{ MeV}, \\ & m_\chi = 596.2 \text{ MeV}, \quad \chi_0 = 254.6 \text{ MeV}; \end{aligned} \quad (18)$$

$$\begin{aligned} \text{set } B: \quad & m_\sigma = 502.7 \text{ MeV}, \quad m_\zeta = 1161.5 \text{ MeV}, \\ & m_\chi = 659.3 \text{ MeV}, \quad \chi_0 = 305.9 \text{ MeV}; \end{aligned} \quad (19)$$

$$\begin{aligned} \text{set } C: \quad & m_\sigma = 466.2 \text{ MeV}, \quad m_\zeta = 1167.1 \text{ MeV}, \\ & m_\chi = 626.4 \text{ MeV}, \quad \chi_0 = 280.2 \text{ MeV}. \end{aligned} \quad (20)$$

All meson masses and the dilaton mass are obtained from the process of chiral symmetry breaking that is density dependent. One can see that the mass of the dilaton is around 600 MeV. In our consideration, we do not identify the dilaton field  $\chi$  with the glueball. It is just an effective field which is related to the glueball via Eq. (10). With the use of transformation (10) in the model Lagrangian, we can obtain the glueball mass  $m_h \approx 1.5$  GeV at  $Z \approx 0.2$  GeV<sup>3</sup>. By the way, both schemes with dilaton field or with glueball are equivalent to each other. A little bit of difference is in the small redefinition of the masses of scalar mesons  $\sigma$  and  $\zeta$ . For example, for set *C*, the Lagrangian with glueball field gives  $m_\sigma = 471.8$  MeV and  $m_\zeta = 1111.6$  MeV.

To check the consistency of our model, it is crucial to estimate the trace anomaly [26,28] which is related to the vacuum expectation value of the dilaton field as

$$\theta_\mu^\mu = (1 - \delta) \chi_0^4. \quad (21)$$

By definition, the trace anomaly of QCD  $\theta_\mu^\mu$  with  $N_f = 3$  (number of flavors) and  $N_c = 3$  (number of colors) is proportional to the gluon condensate:

$$\theta_\mu^\mu = \frac{9}{8} \langle 0 | \frac{\alpha_s}{\pi} G_{\mu\nu}^2 | 0 \rangle. \quad (22)$$

This quantity can be directly estimated with the use of the values of the gluon condensate calculated in QCD [29]:  $(0.006 \pm 0.012)$  GeV<sup>4</sup> taken from analysis of the  $\tau$ -decay data and  $(0.009 \pm 0.007)$  GeV<sup>4</sup> taken from the sum rules for charmonium. The corresponding values of the trace anomaly are  $\theta_\mu^\mu = (0.007 \pm 0.014)$  GeV<sup>4</sup> and  $\theta_\mu^\mu = (0.010 \pm 0.008)$  GeV<sup>4</sup>. Using our average vacuum expectation value  $\chi_0 = 0.28$  GeV, we give the following prediction for the trace anomaly and the gluon condensate:  $\theta_\mu^\mu = 0.005$  GeV<sup>4</sup> and  $\langle 0 | (\alpha_s / \pi) G_{\mu\nu}^2 | 0 \rangle = 0.0045$  GeV<sup>4</sup>. One can see that both values are in agreement with QCD analysis.

### III. APPLICATION TO STRANGE QUARK MATTER

Now we apply the model to investigate strange quark matter. We begin with the thermodynamical potential density because all other quantities such as energy per volume and pressure can be obtained from it. The thermodynamical potential density is defined as

$$\Omega = \sum_{\tau=q,e} \frac{-2k_B T \gamma_\tau}{(2\pi)^3} \int_0^\infty d^3k \{ \ln(1 + e^{-(E_\tau^*(k) - v_\tau)/k_B T}) + \ln(1 + e^{-(E_\tau^*(k) + v_\tau)/k_B T}) \} - \mathcal{L}_M, \quad (23)$$

where  $E_\tau^*(k) = \sqrt{m_\tau^{*2} + k^2}$ ,  $\gamma_\tau$  is 3 for quarks and 1 for electrons and  $\mathcal{L}_M$  is the meson interaction including the scalar meson self-interaction  $\mathcal{L}_{\Sigma\Sigma}$ , the vector meson self-interaction  $\mathcal{L}_{VV}$  and the explicit chiral symmetry breaking term  $\mathcal{L}_{\chi SB}$ . In the MIT bag and the QMDD model,  $\mathcal{L}_M$  is replaced by the effective bag constant. At zero temperature,  $\Omega$  can be expressed as

$$\Omega = - \sum_{i=u,d,s} \frac{1}{8\pi^2} \left\{ v_i [v_i^2 - m_i^{*2}]^{1/2} [2v_i^2 - 5m_i^{*2}] + 3m_i^{*4} \ln \left[ \frac{v_i + (v_i^2 - m_i^{*2})^{1/2}}{m_i^*} \right] \right\} - \frac{\mu_e^4}{12\pi^2} - \mathcal{L}_M, \quad (24)$$

where  $\mu_e$  is the chemical potential of the electron and the quantity  $v_i$  ( $i=u, d, s$ ) is related to the usual chemical potential  $\mu_i$  by  $v_i = \mu_i - g_\omega^i \omega - g_\rho^i \rho - g_\phi^i \phi$ . The effective quark mass is given by  $m_i^* = -g_\sigma^i \sigma - g_\zeta^i \zeta + m_{i0}$ . The total baryon density is defined as

$$\rho_B = \frac{1}{3} (\rho_u + \rho_d + \rho_s). \quad (25)$$

With the thermodynamical potential density, the energy per volume  $\varepsilon$  and pressure  $p$  of the system can be derived as  $\varepsilon = \Omega + \sum_{i=u,d,s,e} \mu_i \rho_i$  and  $p = -\Omega$ .

The mean field equations for the meson  $\phi_i$  are obtained with  $\partial\Omega/\partial\phi_i = 0$ . For the scalar mesons  $\sigma$  and  $\zeta$  and the dilaton field  $\chi$ , the equations are expressed as

$$\begin{aligned} & k_0 \chi^2 \sigma - 4k_1 (\sigma^2 + \zeta^2) \sigma - 2k_2 \sigma^3 - 2k_3 \chi \sigma \zeta - \frac{2\delta}{3\sigma} \chi^4 \\ & + \frac{\chi^2}{\chi_0^2} m_\pi^2 F_\pi - \left( \frac{\chi}{\chi_0} \right)^2 m_\omega \omega^2 \frac{\partial m_\omega}{\partial \sigma} - \left( \frac{\chi}{\chi_0} \right)^2 m_\rho \rho^2 \frac{\partial m_\rho}{\partial \sigma} \\ & = \sum_{i=u,d} g_\sigma^i \langle \bar{\psi}_i \psi_i \rangle, \end{aligned} \quad (26)$$

$$\begin{aligned} & k_0 \chi^2 \zeta - 4k_1 (\sigma^2 + \zeta^2) \zeta - 4k_2 \zeta^3 - k_3 \chi \sigma^2 - \frac{\delta}{3\zeta} \chi^4 \\ & + \frac{\chi^2}{\chi_0^2} \left( \sqrt{2} m_K^2 F_K - \frac{1}{\sqrt{2}} m_\pi^2 F_\pi \right) - \left( \frac{\chi}{\chi_0} \right)^2 m_\phi \phi^2 \frac{\partial m_\phi}{\partial \zeta} \\ & = \sum_{i=s} g_\zeta^i \langle \bar{\psi}_i \psi_i \rangle, \end{aligned} \quad (27)$$

$$\begin{aligned} & k_0 \chi (\sigma^2 + \zeta^2) - k_3 \sigma^2 \zeta + \left( 4k_4 + 1 + 4 \ln \frac{\chi}{\chi_0} - \frac{4\delta}{3} \ln \frac{\sigma^2 \zeta}{\sigma_0^2 \zeta_0} \right) \chi^3 \\ & + \frac{2\chi}{\chi_0^2} \left[ m_\pi^2 F_\pi \sigma + \left( \sqrt{2} m_K^2 F_K - \frac{1}{\sqrt{2}} m_\pi^2 F_\pi \right) \zeta \right] \\ & - \frac{\chi}{\chi_0^2} (m_\omega^2 \omega^2 + m_\rho^2 \rho^2 + m_\phi^2 \phi^2) = 0. \end{aligned} \quad (28)$$

The equations for the vector mesons can be obtained in the same way as

$$\frac{\chi^2}{\chi_0^2} m_\omega^2 \omega + 4g_4 \omega^3 + 12g_4 \omega \rho^2 = \sum_{i=u,d} g_\omega^i \langle \bar{\psi}_i \gamma^0 \psi_i \rangle, \quad (29)$$

$$\frac{\chi^2}{\chi_0^2} m_\rho^2 \rho + 4g_4 \rho^3 + 12g_4 \omega^2 \rho = \sum_{i=u,d} g_\rho^i \langle \bar{\psi}_i \gamma_0 \psi_i \rangle, \quad (30)$$

$$\frac{\chi^2}{\chi_0^2} m_\phi^2 \phi + 8g_4 \phi^3 = \sum_{i=s} g_\phi^i \langle \bar{\psi}_i \gamma_0 \psi_i \rangle. \quad (31)$$

The scalar and vector densities can be written as

$$\langle \bar{\psi}_i \psi_i \rangle = \frac{6}{(2\pi)^3} \int_0^{k_{F_i}} d^3k \frac{m_i^*}{\sqrt{k^2 + m_i^{*2}}}, \quad (32)$$

$$\langle \bar{\psi}_i \gamma^0 \psi_i \rangle = \frac{6}{(2\pi)^3} \int_0^{k_{F_i}} d^3k \quad (33)$$

with  $k_{F_i} = \sqrt{v_i^2 - m_i^{*2}}$ .

### IV. NUMERICAL RESULTS

Now we investigate the implications of the previous formalism to strange quark matter. Compared to earlier applications of hadronic matter, here we need not introduce the confining potential that combines quarks into baryons. In quark matter, the  $u$ ,  $d$ , and  $s$  quarks are deconfined. They only interact by scalar and vector mesons. The self-interactions between mesons are the same as in hadronic matter. All the parameters in this model are determined in our previous papers. They are listed in Table I. The values of meson masses are given in Sec. II. We assume that these parameters do not change when the model is applied to quark matter. In fact, the parameters which describe the interactions between fields “should” be universal. The medium effects are included by



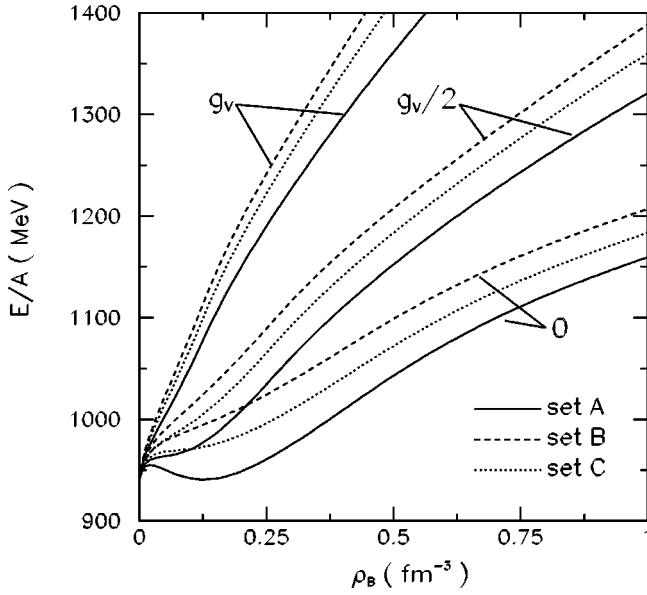


FIG. 1. Energy per baryon versus baryon density for different vector coupling constants. The solid, dashed, and dotted lines are for parameter sets A, B, and C. Results are shown for the case of  $\beta$  equilibrium.

the treatment (relativistic mean field theory) itself and are not included in the original Lagrangian. Earlier investigations based on the MIT bag model [10–15], the QMDD model [17–19], the SU(3) NJL model [23], etc., did not consider the repulsive interaction caused by vector mesons. In Ref. [22], the repulsive vector interaction was included with different strength ( $G_V=0$  and  $G_V=0.5G_S$ ). We will also discuss the stability of strange quark matter with different values for the vector coupling constant. Note that in the SU(3) NJL model with and without vector meson interaction, the chiral symmetry is exactly realized. For comparison, in our discussion, we first do not include the additional coupling  $\mathcal{L}_h$  that breaks chiral symmetry explicitly and discuss the effect of this term on strange quark matter later.

If strange quark matter is stable and can survive for a long time, equilibrium with respect to the weak processes

$$s \rightarrow u + e^- + \bar{\nu}_e, \quad d \rightarrow u + e^- + \bar{\nu}_e \quad (34)$$

may be achieved. If we neglect the chemical potential of the neutrino, the chemical potentials of quarks and electron have the following relation:

$$\mu_d = \mu_s = \mu_u + \mu_e. \quad (35)$$

The values for  $\mu_u$  and  $\mu_d$  are determined by the baryon density and the total charge  $Q$ . As usual, we assume the charge  $Q$  to be zero. Equations (26)–(31) for the mesons can be solved simultaneously. The energy per baryon with a different strength of vector coupling and for different parameter sets are shown in Fig. 1. When vector interactions are not considered, there is a local minimum of energy per baryon with parameter set A. The corresponding density is about  $0.13 \text{ fm}^{-3}$ . As shown later, at this density, no strange quarks appear. When the vector interactions are included, even when

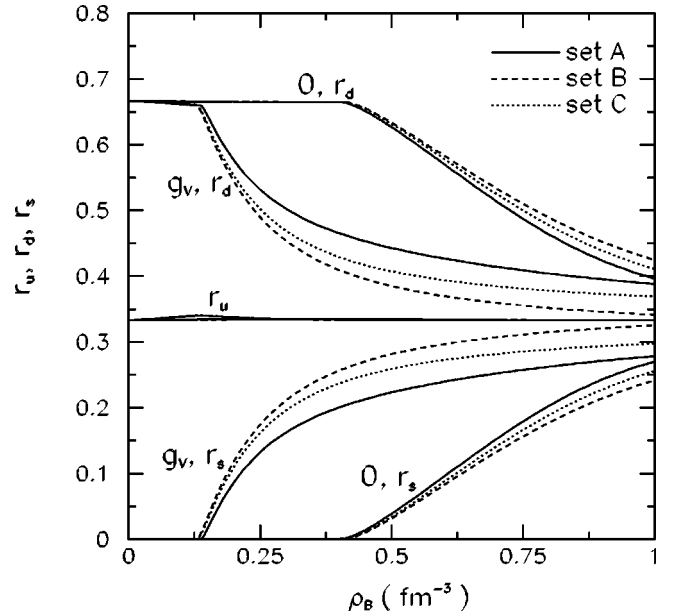


FIG. 2. Fractions of  $u$ ,  $d$ , and  $s$  quarks in strange matter versus baryon density with and without vector interactions, respectively. The solid, dashed, and dotted lines are for parameter sets A, B, and C. Results are shown for the case of  $\beta$  equilibrium.

the strength is half of that in hadronic matter, the local minimum for the energy per baryon disappears. The energy per baryon  $E/A$  increases monotonously with the increasing baryon density.

In Fig. 2, we show the fractions  $r_i = \rho_i/3\rho_B$  of  $u$ ,  $d$ , and  $s$  quark versus baryon density with and without vector interactions. The fraction of  $u$  quarks almost does not change with the density. There exists a relationship  $\rho_d + \rho_s \approx 2\rho_u$ . Therefore, although we included the electron in our calculations, the fraction of electrons is very small. The chemical potential of the electron  $\mu_e$  is not zero which results in a larger fraction of  $d$  than  $u$  quarks. At low density, no strange quarks are present. The fraction of  $d$  quarks is about 2 times that of  $u$  quarks. Without vector interactions, when the density is larger than about  $0.41 \text{ fm}^{-3}$ , strange quarks appear. Compared to Fig. 1, this density is larger than the density where the local minimum appears. This result is consistent with that of Ref. [23], where the SU(3) NJL model was used. In that model, the strange quark appears when the baryon density is about  $4\rho_0$  ( $\rho_0$  is the saturation density of symmetric nuclear matter), while the minimum of energy per baryon occurs at  $\rho \approx 2.5\rho_0$ . Therefore, no stable strange quark matter can exist at zero pressure. The so-called strange star cannot be composed entirely by the deconfined  $u$ ,  $d$ , and  $s$  quarks. The stable strange quark matter can only exist in the core of these objects where the pressure is high enough to force the transition from hadronic matter to quark matter to occur.

If strange quark matter is metastable, then it may be produced in heavy-ion collisions. In this case, the  $\beta$  equilibrium may not be achieved. In our calculations, we assume that  $\mu_u = \mu_d = \mu_q$ . The values of  $\mu_q$  and  $\mu_s$  are determined by the total baryon density and the strangeness fraction  $f_s$  ( $f_s = 3r_s$ ). In Fig. 3, we plot the effective masses of nonstrange and strange quarks versus the baryon density for different

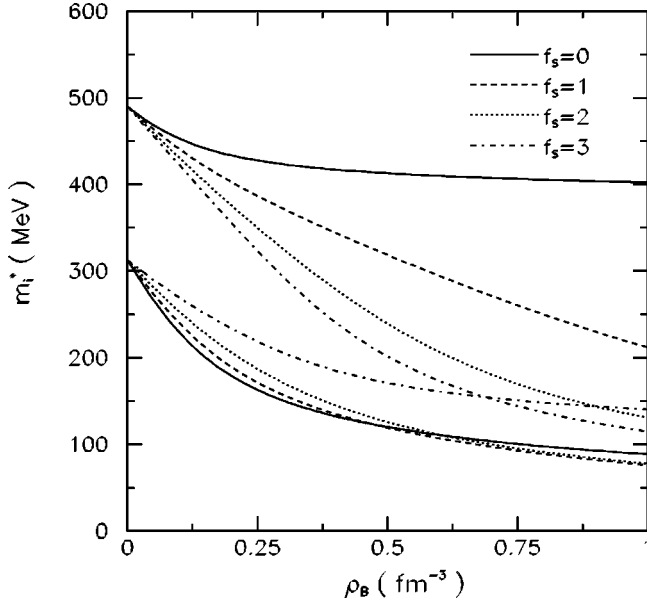


FIG. 3. The effective nonstrange and strange quark masses versus baryon density for different strangeness fraction. Parameters are taken from set C.

strangeness fractions with parameter set C. Both  $u$  ( $d$ ) and  $s$  quark masses decrease with the increasing density. In nonstrange quark matter, the mass of the  $u$  ( $d$ ) quark decreases more quickly than that of the  $s$  quark. When  $f_s$  increases, the mass of the  $s$  quark decreases at a fixed density. At some high density, the strange quark mass is even lower than the mass of nonstrange quarks. Compared to the QMDD model, here the effective quark masses are obtained dynamically. The quark masses are not only density dependent but also strangeness fraction dependent which are not present in the QMDD model. The density and strangeness dependence of the quark masses is close to that of Ref. [22] calculated in the SU(3) NJL model.

The chiral symmetry restoration can be studied from the quark condensates. The nonstrange and strange quark condensates are shown in Fig. 4 for both bulk matter in  $\beta$  equilibrium and metastable matter with  $f_s=0$  and  $f_s=3.0$ . For the case of  $f_s=0$ , the nonstrange quark condensate  $\sigma/\sigma_0$  decreases faster than the strange quark condensate  $\zeta/\zeta_0$  with the increasing baryon density. At the density  $\rho_B=\rho_0$ ,  $\rho_B=2\rho_0$ , and  $\rho_B=3\rho_0$ ,  $\sigma/\sigma_0$  is about 0.6, 0.5, and 0.38. At low density, the quark condensate can be expanded as [30]

$$\frac{\langle \bar{q}q \rangle_\rho}{\langle \bar{q}q \rangle_0} = 1 - \frac{\sigma_N}{f_\pi^2 m_\pi^2} \rho, \quad (36)$$

where  $\sigma_N$  is the nucleon sigma term. The above equation suggests about 30% reduction in the quark condensate at nuclear saturation density. When density is smaller than  $2\rho_0$ , our result is close to that of NJL model [31]. At higher density, NJL model gives lower quark condensate. When the  $f_s$  increases, the value of  $\zeta/\zeta_0$  decreases evidently. The density dependence of nonstrange quark condensate changes a little when  $f_s < 2.0$ . For any number of  $f_s$ , the value of  $\sigma/\sigma_0$  is

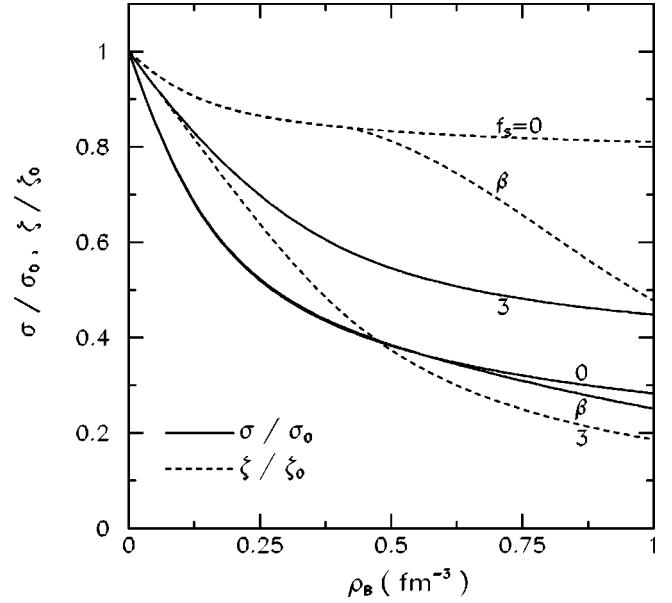


FIG. 4. The nonstrange and strange quark condensates versus baryon density for different strangeness fraction. Parameters are taken from set C.

smaller than 0.5 at high baryon density. For the case of  $\beta$  equilibrium, the density dependence of quark condensates is the same as in the case of  $f_s=0$  at low density. This is because at low density, no strange quarks appear which can be seen in Fig. 2. At  $\rho_B \approx 0.41 \text{ fm}^{-3}$ , the strange quarks appear. As a result,  $\zeta/\zeta_0$  will be smaller than that with  $f_s=0$ . The nonstrange quark condensate changes a little because  $f_s$  of the system in  $\beta$  equilibrium is smaller than 1. The density dependence of the quark condensates determines the energy per baryon of the system through the effective quark masses. For the system in  $\beta$  equilibrium, the small decrease of strange quark condensate results in the small decrease of the effective strange quark masses. For the metastable strange quark matter with large strangeness fraction, the large decrease of strange quark condensate can produce a sizable binding energy.

In Figs. 5–7, we plot the energy per baryon versus density for different values of  $f_s$ , which corresponds to different vector coupling constants. The solid, dashed, and dotted lines are for parameter sets A, B, and C, respectively. First, we do not include the interactions between quarks and vector mesons. This is close to the QMDD model or the SU(3) NJL model with only scalar-type 4-quark interactions. In Fig. 5, for parameter set A, there exists a local minimum of energy per baryon for any  $f_s$ . The baryon density at the minimum of energy per baryon first increases and then decreases when  $f_s$  increases. For nonstrange quark matter, though there is a local minimum, the system has no positive binding energy compared to the vacuum mass of nonstrange quarks. For strange quark matter, the energy per baryon is lower than the masses of hyperons with the same strangeness number. When  $f_s=1$ , the binding energy is about 45 MeV compared to the vacuum constituent quark mass. The maximum binding energy is about 60 MeV and the corresponding  $f_s$  is about 2.0. Metastable strange quark matter is, therefore, fa-

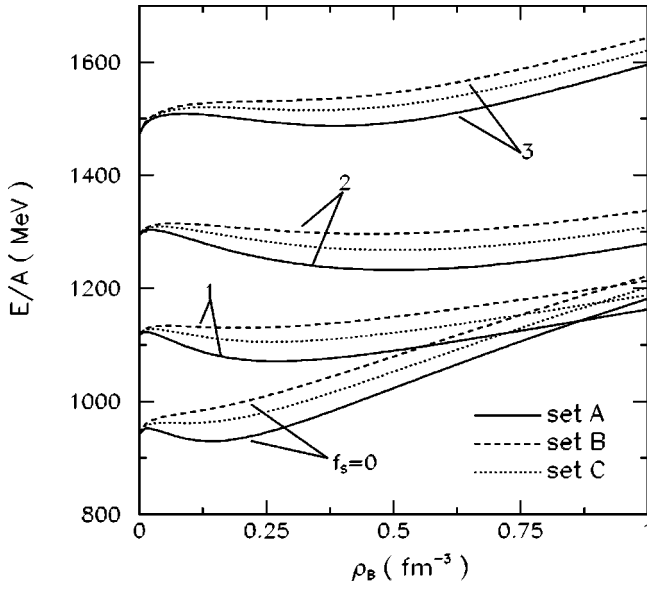


FIG. 5. The energy per baryon versus baryon density for different strangeness fraction for parameter sets A, B, and C. The interaction between quarks and vector mesons is not considered.

vored to have a large strangeness fraction (high negative charge). For the parameter set B, the system has a local minimum of energy per baryon only for some range of  $f_s$ , that is  $1 < f_s < 3$ . The maximum binding energy is about 5 MeV when  $f_s$  is around 2.0. The result of parameter set C is between those of sets A and B. Our result is comparable to the one in Ref. [22], where the maximum binding energy is about 90 MeV and the corresponding strangeness fraction is around 1.7 in the case of  $G_V = 0$ .

When the interactions between quarks and vector mesons are included, the system is destabilized. In Fig. 6, we plot the

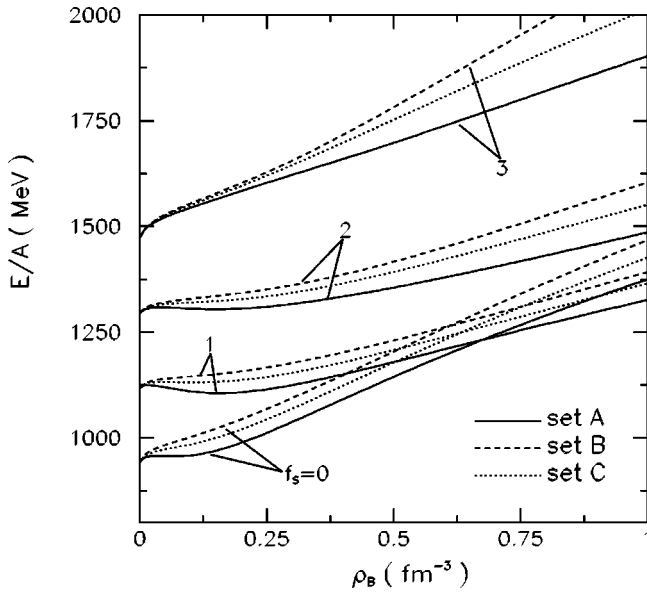


FIG. 6. Same as in Fig. 5, but here the quark-vector meson interaction is included. The value of the vector coupling constant is half of that for hadronic matter.

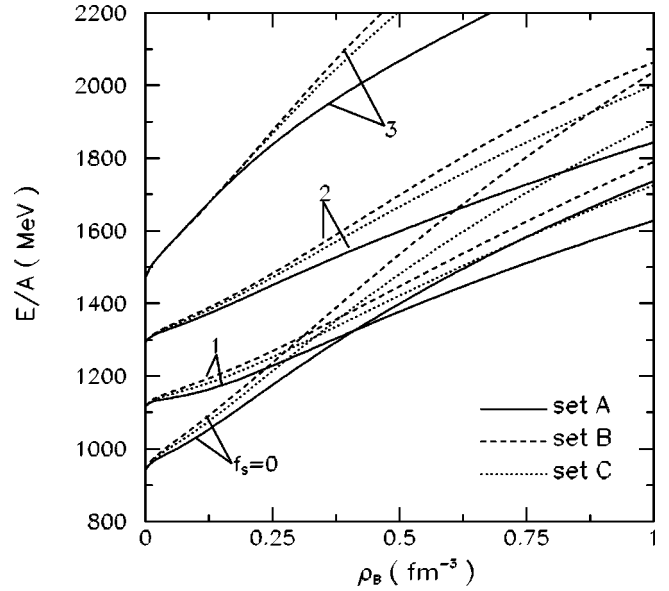


FIG. 7. Same as Fig. 5, but the vector coupling constant is of the strength as in hadronic matter.

energy per baryon versus baryon density with the vector coupling constant half of that in hadronic matter. Compared to Fig. 5, the energy per baryon becomes higher. For parameter set A, there exists a local minimum for  $0 < f_s < 2$ . The maximum binding energy is only about 10 MeV with  $f_s \approx 1.0$ . The corresponding density is also much lower compared to Fig. 5. For parameter sets B and C, there is no local minimum for any strangeness fraction. If the vector coupling is the same as in hadronic matter, as is shown in Fig. 7, the energy per baryon will increase monotonously with the baryon density for all parameter sets. The vector meson couplings are also discussed in Ref. [22]. When  $G_V = 0.5G_S$ , strange quark matter is found to have a positive binding energy for  $0.6 < f_s < 1.6$  and the maximum binding energy is about 15 MeV at  $f_s \approx 1.2$ .

Therefore, if vector interactions are included, even when the strength is only half of that in hadronic matter, the binding energy of metastable strange quark matter becomes small or negative. At the minimum of the energy per baryon, the pressure  $p$  of the system is zero. This kind of objects with finite volume are called strangelets. If the vector interactions are fully considered, the metastable strangelets cannot be formed at zero pressure.

Up to now, we did not consider the additional coupling between strange quark and scalar mesons  $\mathcal{L}_h$ , which is important to obtain reasonable hyperon potentials in hadronic matter [24]. When the additional term is included, the effective quark masses versus baryon density for parameter set C are given in Fig. 8. The result for the strange quark mass evidently change, especially for large strangeness fraction, when compared to Fig. 3. In nonstrange quark matter, the effective mass of  $s$  quarks almost stays constant. When the strangeness fraction is high, the strange quark has a lower mass when compared to Fig. 3, where  $\mathcal{L}_h$  is not included.

The effective quark masses will affect the energy of the system. In Figs. 9 and 10, we plot the energy per baryon

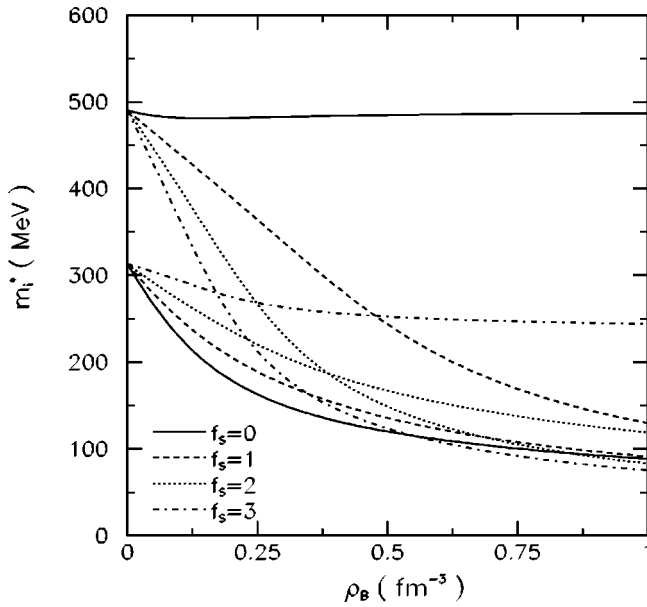


FIG. 8. Same as Fig. 3, but the the additional term  $\mathcal{L}_h$  is included in the calculation.

versus density for different vector coupling constant with parameter set  $C$ . The solid and dashed lines correspond to the cases without and with  $\mathcal{L}_h$ , respectively. For small strangeness fraction  $f_s$ , the results of these two cases are close. For large strangeness fraction, the additional term  $\mathcal{L}_h$  will produce larger binding energy. Without the vector meson interaction (Fig. 9), the binding energy is now about 100 MeV when  $f_s$  is larger than 2. The corresponding saturation density is around  $2-3\rho_0$ . In Fig. 10, the vector coupling is half of that for hadronic matter. The additional term  $\mathcal{L}_h$  makes the energy per baryon decrease when the strangeness fraction is

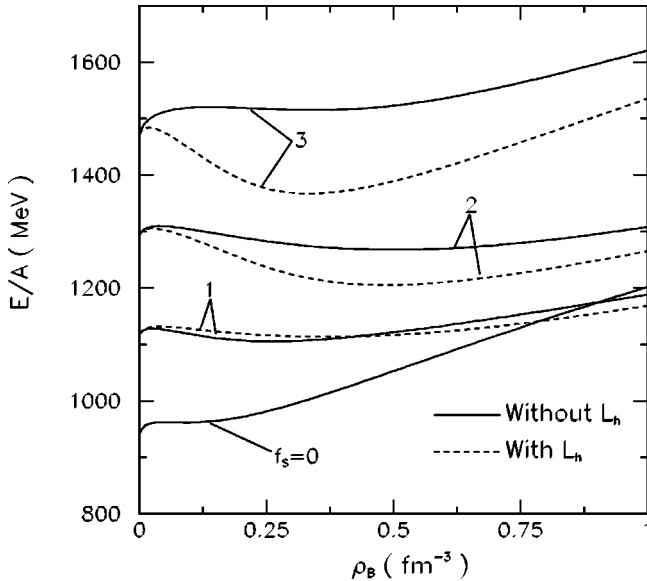


FIG. 9. The energy per baryon versus baryon density for parameter set  $C$  without vector meson interaction. Solid and dashed lines correspond to the case without and with the additional term  $\mathcal{L}_h$ , respectively.

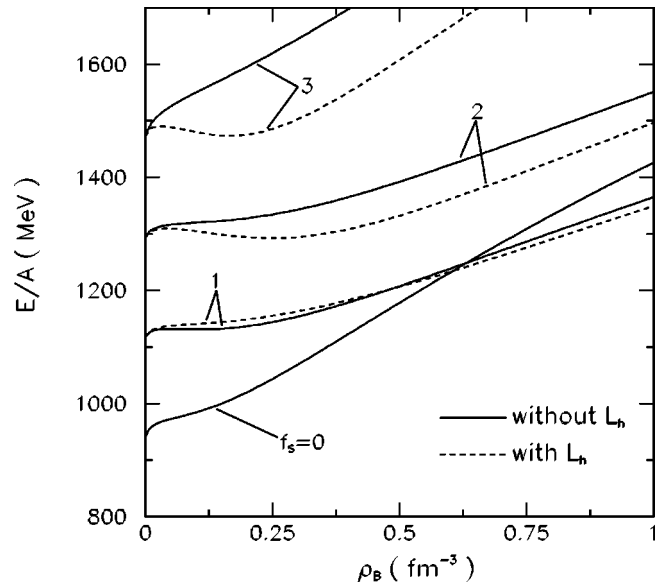


FIG. 10. Same as Fig. 9, but the vector coupling constant is half of that for hadronic matter.

high. The strange quark matter still can be weakly bound with some high strangeness fractions in this case. If the vector coupling strength is as large as in hadronic matter, there is no local minimum for both cases, with or without  $\mathcal{L}_h$ . For the case when the  $\beta$  equilibrium is achieved, the strangeness fraction of the system is smaller than 1. The additional term  $\mathcal{L}_h$  only gives sizable contributions for systems with a large strangeness fraction. Therefore, the inclusion of the additional term  $\mathcal{L}_h$  does not affect the main results of Fig. 1.

To see clearly the binding energy of the system with different strangeness fraction, in Fig. 11, we plot the binding

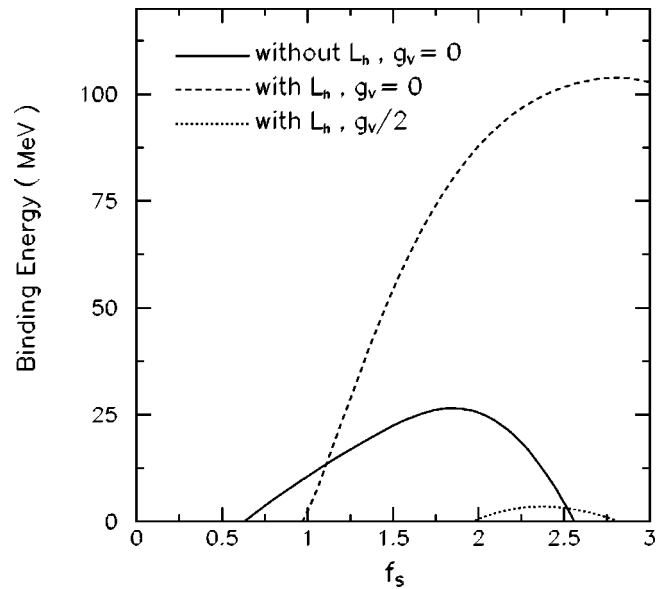


FIG. 11. The binding energy of the system versus strangeness fraction with parameter set  $C$ . The solid, dashed, and dotted lines correspond to the case without additional term  $\mathcal{L}_h$  and vector meson coupling  $g_v$ , with  $\mathcal{L}_h$  and without  $g_v$ , and with  $\mathcal{L}_h$  and  $g_v$ , respectively.



energy versus  $f_s$  with parameter set  $C$  which is better for hadronic matter compared with sets  $A$  and  $B$ . One can see that without the additional term  $\mathcal{L}_h$  and vector meson interactions, strange quark matter has a positive binding energy for  $0.6 < f_s < 2.6$ . The maximum binding energy is about 25 MeV and the corresponding strangeness fraction is about 1.9. If the vector coupling constant is half of that in hadronic matter, the system has no positive binding energy. When  $\mathcal{L}_h$  is included, the system can be self-bound when  $f_s > 1$ . The maximum binding energy is about 102 MeV with  $f_s = 2.8$ . Strange quark matter can still be weakly bound when  $2 < f_s < 2.6$  if vector coupling is half of that in hadronic matter.

## V. CONCLUSIONS

We investigate strange quark matter in a chiral SU(3) quark mean field model. The effective quark masses are obtained dynamically by the quark meson interactions and they are both density and strangeness fraction dependent. The stability of strange quark matter is studied for different values of the vector coupling constant and for different parameter sets. The effect of the additional term  $\mathcal{L}_h$  is also discussed.

In the case where  $\beta$  equilibrium is achieved, the strangeness fraction  $f_s$  of quark matter is smaller than 1. In the chiral SU(3) quark model, at the density where the system has a local minimum for the energy per baryon, no strange quarks appear. Even without the vector meson coupling, this nonstrange quark matter has a negative binding energy and cannot be self-bound. Therefore, opposed to the early suggestion [1,2], stable quark matter at zero pressure cannot exist even without vector meson interactions.

If quark matter can be produced in heavy-ion collisions,

the  $\beta$  equilibrium may not be achieved. This metastable strange quark matter can have a high strangeness fraction (high negative charge). When we do not take the vector meson interaction into account, as in the QMDD model or the SU(3) NJL model with only scalar-type four-quark interaction, the maximum binding energy is about 5–60 MeV and the corresponding strangeness fraction is about 1–2 for different parameter sets. If we assume that the strength of vector meson coupling is half of that in hadronic matter (in this case, the strength of vector coupling is comparable to the one of Ref. [22]), the maximum binding energy decreases. Inclusion of the additional term  $\mathcal{L}_h$  will force the system to have a larger strangeness fraction and binding energy. When the vector coupling constant is the same as for hadronic matter, no metastable strange quark matter (strangelets) can be formed in heavy-ion collisions.

However, strange quark matter can still exist in the core of a neutron star. The phase transition from hadronic matter to quark matter can occur at high density and pressure which is caused by gravity. This kind of phase transition has been studied by numerous papers starting from the 1970s (see, for example, Ref. [32]). Because both hadronic and quark matter can be described in the SU(3) quark mean field model, it is of interest to investigate this phase transition in this model. This will be studied in the future.

## ACKNOWLEDGMENTS

P.W. would like to thank the Institute for Theoretical Physics, University of Tübingen for their hospitality. This work was supported by the Alexander von Humboldt Foundation and by the Deutsche Forschungsgemeinschaft (DFG) under Contract Nos. FA67/25-1 and GRK683.

- 
- [1] A.R. Bodmer, Phys. Rev. D **4**, 1601 (1971).
  - [2] E. Witten, Phys. Rev. D **30**, 272 (1984).
  - [3] M. Kasuya *et al.*, Phys. Rev. D **47**, 2153 (1993); M. Ichimura *et al.*, Nuovo Cimento Soc. Ital. Fis., A **106**, 843 (1993); J.N. Capdevielle *et al.*, Nuovo Cimento Soc. Ital. Fis., C **19**, 623 (1996).
  - [4] K.S. Cheng, Z.G. Dai, D.M. Wai, and T. Lu, Science **280**, 407 (1998).
  - [5] X.D. Li, I. Bombaci, M. Dey, J. Dey, and E.P.J. van den Heuvel, Phys. Rev. Lett. **83**, 3776 (1999).
  - [6] C. Greiner, D.H. Rischke, H. Stöcker, and P. Koch, Phys. Rev. D **38**, 2797 (1988).
  - [7] J. Barrette *et al.*, Phys. Lett. B **252**, 550 (1990); M. Aoki *et al.*, Phys. Rev. Lett. **69**, 2345 (1992); K. Borer *et al.*, *ibid.* **72**, 1415 (1994); D. Beavis *et al.*, *ibid.* **75**, 3078 (1995).
  - [8] D. Ardouin *et al.*, Phys. Lett. B **446**, 191 (1999).
  - [9] T.A. Armstrong *et al.*, Phys. Rev. C **59**, 1829 (1999); **63**, 054903 (2001).
  - [10] A. Chodos *et al.*, Phys. Rev. D **9**, 3472 (1974).
  - [11] E. Farhi and R.L. Jaffe, Phys. Rev. D **30**, 2379 (1984).
  - [12] S.A. Chin and A.K. Kerman, Phys. Rev. Lett. **43**, 1292 (1979).
  - [13] M.S. Berger and R.L. Jaffe, Phys. Rev. C **35**, 213 (1987).
  - [14] J. Schaffner, C. Greiner, A. Diener, and H. Stöcker, Phys. Rev. C **55**, 3038 (1997).
  - [15] J. Madsen, Phys. Rev. Lett. **70**, 391 (1993); Phys. Rev. D **47**, 5156 (1993).
  - [16] A. Ukawa, Nucl. Phys. **A498**, 227c (1989).
  - [17] G.N. Fowler, S. Raha, and R.M. Weiner, Z. Phys. C **9**, 271 (1981).
  - [18] S. Chakrabarty, S. Raha, and B. Sinha, Phys. Lett. B **229**, 112 (1989); O.G. Benvenuto and G. Lugones, Phys. Rev. D **51**, 1989 (1995).
  - [19] P. Wang, Phys. Rev. C **62**, 015204 (2000).
  - [20] W.M. Alberico, A. Drago, and C. Ratti, Nucl. Phys. **A706**, 143 (2002).
  - [21] M. Jaminon and B. Van den Bossche, Nucl. Phys. **A686**, 341 (2001).
  - [22] I.N. Mishustin, L.M. Satarov, H. Stöcker, and W. Greiner, Phys. At. Nucl. **64**, 802 (2001).
  - [23] M. Buballa and M. Oertel, Phys. Lett. B **457**, 261 (1999).
  - [24] P. Wang, Z.Y. Zhang, Y.W. Yu, R.K. Su, and H.Q. Song, Nucl. Phys. **A688**, 791 (2001).
  - [25] P. Wang, H. Guo, Z.Y. Zhang, Y.W. Yu, R.K. Su, and H.Q. Song, Nucl. Phys. **A705**, 455 (2002).
  - [26] P. Papazoglou, D. Zschesche, S. Schramm, J. Schaffner-Bielich, H. Stöcker, and W. Greiner, Phys. Rev. C **59**, 411 (1999).

- [27] H. Gomm, P. Jain, R. Robson, and J. Schechter, Phys. Rev. D **33**, 801 (1986).
- [28] J. Schechter, Phys. Rev. D **21**, 3393 (1980).
- [29] B.L. Ioffe, hep-ph/0207191.
- [30] L.S. Celenza, C.M. Shakin, Wei-Dong Sun, and Xiquan Zhu, Phys. Rev. C **48**, 159 (1993).
- [31] I.N. Mishustin, L.M. Satarov, H. Stöcker, and W. Greiner, Phys. Rev. C **62**, 034901 (2000).
- [32] J.C. Collins and M.J. Perry, Phys. Rev. Lett. **34**, 1353 (1975); G. Baym and S.A. Chin, Phys. Lett. **62B**, 241 (1976).